CHEMISTRY OF MATERIALS

pubs.acs.org/cm

Article

# Optimizing the Thermodynamics and Kinetics of the Triplet-Pair Dissociation in Donor–Acceptor Copolymers for Intramolecular Singlet Fission

Maria Fumanal and Clémence Corminboeuf*

Cite This: *Chem. Mater.* 2022, 34, 4115–4121

Read Online

ACCESS | Metrics & More | Article Recommendations | Supporting Information

**ABSTRACT:** Singlet fission (SF) is a two-step process in which a singlet splits into two triplets throughout the so-called correlated triplet-pair ($^1$TT) state. Intramolecular SF (iSF) materials, in particular, have attracted growing interest as they can be easily implemented in single-junction solar cells and boost their power conversion efficiency. Still, the potential of iSF materials such as polymers and oligomers for photovoltaic applications has been partially hindered by their ability to go beyond the $^1$TT intermediate and generate free triplets, whose mechanism remains poorly understood. In this work, the main aspects governing the $^1$TT dissociation in donor–acceptor copolymers and the key features that optimize this process are exposed. First, we show that both thermodynamics and kinetics play a crucial role in the intramolecular triplet-pair separation and second, we uncover the inherent flexibility of the donor unit as the fundamental ingredient to optimize them simultaneously. Overall, these results provide a better understanding of the intramolecular $^1$TT dissociation process and establish a new paradigm for the development of novel iSF active materials.

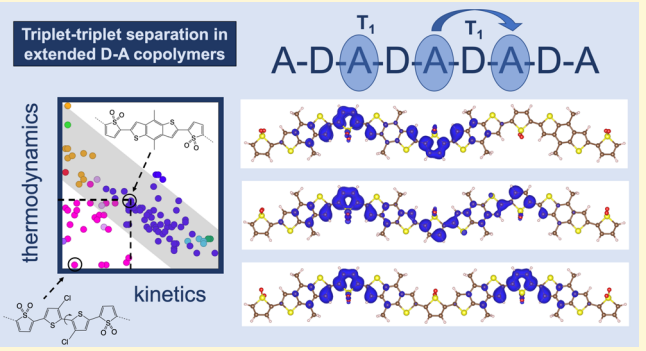


## INTRODUCTION

Singlet fission (SF) is the photophysical phenomenon in which a singlet state is converted into two independent triplets. This occurs via the so-called correlated triplet-pair state ($^1$TT), which belongs to the singlet state manifold and thus can be accessed through a spin-allowed reaction. Once the $^1$TT state is formed, it dissociates into two triplet excitons to complete the process (eq 1).[1−3]

$$S_1 \rightarrow {}^1\mathrm{TT} \rightarrow 2T_1 \quad (1)$$

Materials exhibiting SF have received significant interest for applications in photovoltaics because of their potential to overcome the thermodynamic Shockey–Queisser 33% limit of single-junction solar cells and boost their power conversion efficiency up to 45%.[4−6] The challenge of finding SF materials comes from designing chromophores that fulfill not only the energetics $E(S_1) \geq 2E(T_1)$ but also undergo fast singlet splitting and triplet-pair dissociation rates. Anthracene[7] and tetracene[8] were the first molecular crystals in which SF was identified. Since then, extensive experimental[9−14] and theoretical[15−19] work on acene derivatives has significantly pushed the understanding of the SF process. However, the poor photostability of these systems and their limitations for practical implementations has urged the search for more diverse SF-active materials.[20−22] In this context, other families of SF materials such as carotenoids[23] and conjugated polymers[24,25] have been considered, although so far to a much less extent. The one-dimensional sequence of chromophores in extended polymers opens the possibility of iSF through their characteristic lowest singlet excited state of a multiexciton character.[26−28] This feature, together with their high tunability and easy processability, makes conjugated polymers particularly attractive for the development of novel iSF materials. In particular, Busby et al. proposed a push–pull donor–acceptor (D–A) copolymer framework to obtain highly efficient iSF.[29] In this strategy, optical absorption promotes D-to-A charge transfer (CT) sideways that drives the formation of two low-lying spatially separated triplets localized in the acceptor units (Figure 1). Remarkable triplet quantum yields up to 170% were reported for poly(benzodithiophene-*alt*-thiophene-1,1-dioxide) (BDT-TDO) polymer chains in solution as well as for similar D–A copolymers following the same approach.[24,30,31] Still, only very few conjugated polymers fulfill the criteria for iSF, namely, energetics and coupling

Received: February 4, 2022
Revised: March 9, 2022
Published: April 21, 2022

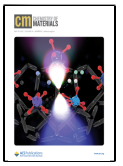





https://doi.org/10.1021/acs.chemmater.2c00367
*Chem. Mater.* 2022, 34, 4115–4121

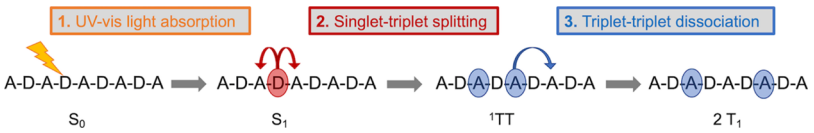


**Figure 1.** Schematic representation of the iSF steps in D−A copolymers. First, UV−vis light absorption promotes $S_0$ to $S_1$, characterized by strong D-to-A CT sideways. Second, $S_1$ decays via a spin-allowed process toward the triplet-pair state $^1$TT, localized in adjacent A. Third, the $^1$TT state spatially dissociates and become two independent $T_1$ triplets.

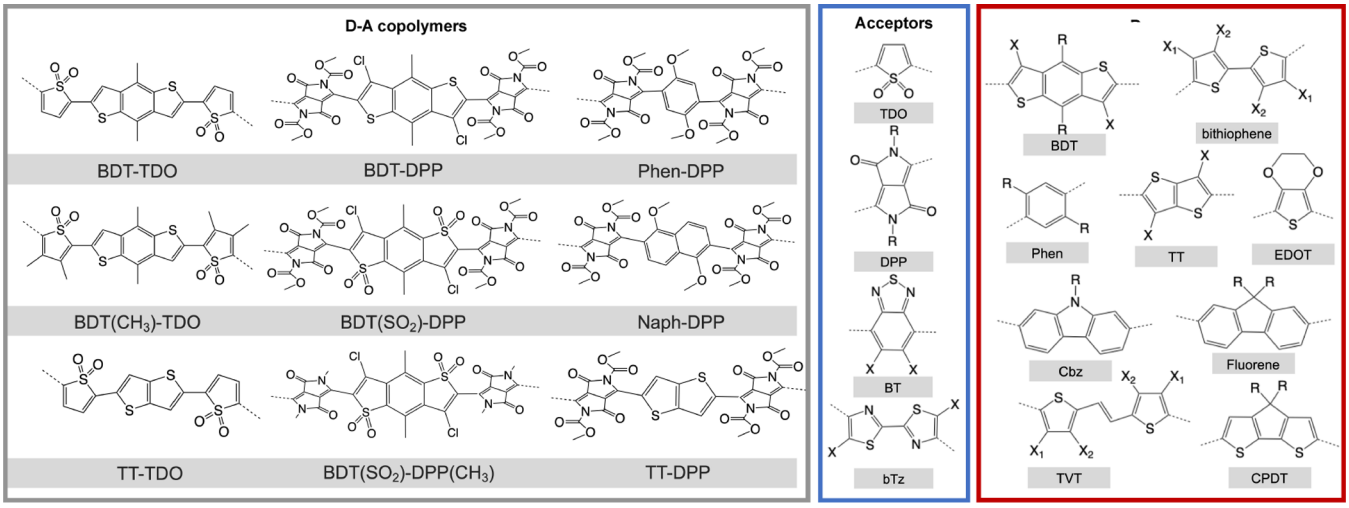


**Figure 2.** Left: nine D−A copolymers considered for extended (5A and 4A) models. Right: library of donors and acceptors of the database of 100 A−D−A trimers (2A model) considered, extracted from ref 32. R groups include H, Me, OMe, and COOMe, and X groups include H, F, Cl, CN, and OH. Acronyms: thiophene-1,1-dioxide (TDO), diketopyrrolopyrrole (DPP), benzothiadiazole (BT), 2,2-bithiazole (bTz), benzodithiophene (BDT), phenylene (Phen), thieno[3,2]thiophene (TT), ethylenedioxythiophene (EDOT), carbazole (Cbz), thiophene-vinyl-thiophene (TVT), cyclopentadithiophene (CPDT), naphthalene (Naph).

requirements. Indeed, a fundamental trade-off between the ability to display D-to-A CT $S_1$ and acceptor-local $T_1$ in coplanar copolymers was identified,[32] evidencing the need for accelerated design strategies to find promising SF candidates.[33,34] A comprehensive structure−property analysis of D−A copolymers allowed us to recognize the role of dihedral torsion in modulating and pushing the CT and local character of the excitations beyond the limit of the coplanar approach.[32,35] On the one side, a larger CT resulted in larger $S_1$/$^1$TT electronic coupling in a series of modified TDO-based copolymers, promoting fast $S_1$-to-$^1$TT dynamics.[28] On the other side, localized $T_1$ in the acceptor reduces the $^1$TT binding energy (evaluated as the vertical energy difference with the $^5$TT state), which is traditionally associated with better triplet−triplet dissociation rates.[36]

The loss of spin coherence between the triplets and the triplet-pair separation process are crucial steps for the successful implementation of SF copolymer materials in solar cell devices.[37,38] In this context, theoretical frameworks have been recently developed to model triplet-pair dissociation in acene-based molecular crystals.[39,40] Still, the triplet-pair dissociation process in D−A copolymers remains unexplored. In this work, we show that considering the $^1$TT binding energy is not enough to anticipate favorable intramolecular triplet−triplet dissociation rates in D−A copolymers. For a series of extended prototypes (Figure 2), we evaluate the TT, $2T_1$, and intermediate structures and uncover that not only the $^1$TT dissociation thermodynamics but also the intramolecular triplet transport kinetics play an important role in the triplet-pair separation process. We discuss whether it is possible and how to optimize both features simultaneously and propose a simple model based on sequential $T_1$ potentials to rationalize and predict their behavior.

## METHODS

Initial structures of the D−A copolymers were obtained from the SMILES-to-*xyz* transformation given by Openbabel with the MMFF94 force field.[41] Geometry optimization of the ground state singlet, $T_1$, TT, and $2T_1$ electronic states was performed on top with the $\omega$B97X-D[42] functional and 6-31g(d) basis set using Gaussian 09 (D.01).[43] The TT and $2T_1$ geometries were obtained for the quintuplet spin state with unrestricted DFT. Three different extended models were considered: 5-acceptors (5A) model with sequence A−D−A−D−A−D−A−D−A, 4-acceptors (4A) model with sequence A−D−A−D−A−D−A, and 2-acceptors (2A) model with sequence A−D−A. Transition state (or intermediate) geometries of the $^5$TT → $2T_1$ reaction were obtained with the 5A model starting from the linear interpolation between the A−D−$T_1$−D−$T_1$−D−A−D−A (TT) and A−D−$T_1$−D−A−D−$T_1$−D−A ($2T_1$) geometries. Transition state (or intermediate) geometries of the $T_1$ → $T_1$ reaction were obtained with the 4A (2A) model starting from the linear interpolation between the A−D−$T_1$−D−A−D−A ($T_1$−D−A) and A−D−A−D−$T_1$−D−A (A−D−$T_1$) geometries. Frequency computations confirmed the nature of the critical points as minimum or transition states of the potential energy surface.

Non-collinear spin-flip TDDFT[44] (with the $\omega$B97X-D functional) and restricted active space spin-flip RAS-2SF[45] computations, both with 6-31g(d), were performed on top of the optimized TT and $2T_1$ 5A model geometries (A−D−$T_1$−D−$T_1$−D−A−D−A and A−D−$T_1$−D−A−D−$T_1$−D−A) to determine the $^5$TT−$^3$TT−$^1$TT vertical energy splitting and the $^{1,3,5}$TT → $2T_1$ reaction energies using Q-Chem 5.1.[46] Extended computational details, including basis set and functional benchmarking, can be found in Sections S1−S4 of the Supporting Information.


https://doi.org/10.1021/acs.chemmater.2c00367
Chem. Mater. 2022, 34, 4115−4121

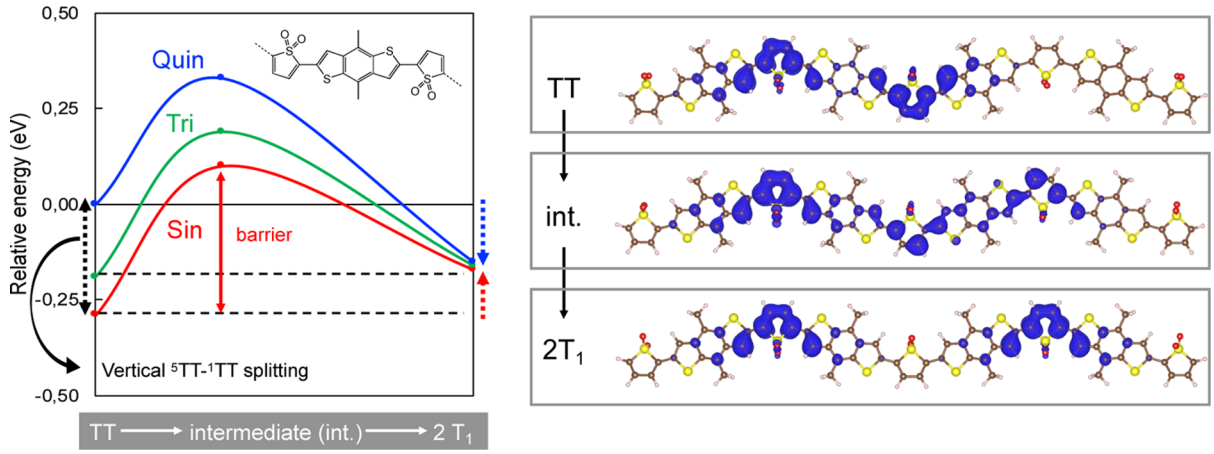


**Figure 3.** Left: representation of the TT dissociation profile. From left to right of the graph: TT, intermediate, and $2T_1$ geometry of the 5A model of the BDT-TDO copolymer. Singlet, triplet, and quintuplet energies computed with SF-TDDFT. On TT geometry (left) is indicated the vertical energy difference between $^5$TT and $^1$TT (otherwise known as the TT binding energy). On the $2T_1$ geometry (right), the negative and positive dissociation energy of the $^5$TT (blue) and $^1$TT (red) states, respectively, is indicated. The middle (intermediate) geometry point corresponds to the minimum energy intermediate along the linear path between $^5$TT and $2T_1$. Right: quintuplet spin density isosurface (0.002 cutoff) of the three minima.

## RESULTS AND DISCUSSION

The TT binding energy is considered the minimal energy required for the separation of the triplet-pair and is usually evaluated as the $^5$TT−$^1$TT vertical energy difference, as it is related to the degree of electronic configuration mixing of the TT states.[15,36,47] On the one side, the mixing of the $^5$TT state is limited because the other quintuplet configurations are much higher in energy; thus, it is used as a proxy of two non-interacting triplets ($2T_1$). On the other side, electronic interaction between the triplets becomes large in $^1$TT when other singlet configurations significantly contribute to stabilize its energy. This is usually the case in extended conjugated systems such as polymers where the characteristic low-lying multi-excitonic singlet is strongly mixed with the lowest mono-electronic transition of the same symmetry.[48,49] In a previous work, we showed how the TT binding energy can be reduced in A−D−A trimers by means of inducing dihedral torsion between the D and A molecular building blocks,[35] therefore potentially accelerating the triplet-pair dissociation rates in agreement with the model established for SF dimers.[36,47] Still, it is unknown whether this model applies to extended D−A copolymers and more importantly which features control the intrachain triplet-pair dissociation process in these systems. To address this question, the triplet−triplet dissociation scenario of the BDT-TDO coplanar prototype was evaluated (Figure 3 and Section S5). To do so, the relative energy between the TT and $2T_1$ geometries was computed in the singlet, triplet, and quintuplet states as well as the minimum energy barrier between the two structures. Both $^5$TT and $^1$TT spin states result in non-zero dissociation energies. In the case of $^5$TT the dissociation energy to $2T_1$ is negative (−0.18 eV), indicating repulsive interaction between the triplets, while for $^1$TT, the dissociation energy is positive (+0.13 eV), indicating attraction. Near zero dissociation energy is obtained for $^3$TT (+0.03 eV). Remarkably, the three spin states display similar barrier energies whose value (∼0.3 eV) is significantly larger than the $^1\text{TT} \rightarrow 2T_1$ reaction energy, thus indicating that the kinetics would control the rate of the TT dissociation process over the thermodynamics. Note that the $2T_1 \rightarrow$ TT process is also possible. There will be inevitable triplet−triplet re-encounters along the copolymer chain assuming long $T_1$ lifetimes, leading to an effective equilibrium between $2T_1$, TT, and $S_1$ states. Analysis of the spin density of the TT, intermediate, and $2T_1$ structures shows that the dissociation is mainly characterized by the energy transfer of one $T_1$ from one acceptor to another passing throughout a donor unit (Figures 3 and S5.1). This anticipates that intrachain triplet transport is a crucial step in the triplet−triplet dissociation reaction of iSF in D−A copolymers.

The same analysis was performed for the BDT-DPP non-coplanar prototype (Figure 2 and Section S6). This D−A copolymer displays a significant dihedral torsion (∼60°) between the donor and acceptor units due to the steric repulsion between their functional groups and, as a consequence, reduces the $^5$TT−$^1$TT splitting down to ∼0 eV.[35] In agreement with this result, the computed TT-to-$2T_1$ reaction energies of the extended chain are close to 0 eV regardless of the spin state (Table S6.1). The dissociation barrier, however, increases up to ∼0.5 eV for the minimum energy intermediate that connects both structures (Figure S6.1). Therefore, while the $^1$TT dissociation thermodynamics of BDT-DPP is more favorable than that of BDT-TDO, the triplet dissociation kinetics would slow down. Indeed, the electronic entropy of the $^1\text{TT} \rightarrow 2T_1$ process is ∼0.3 eV, and thus, barriers or dissociation energies above this value would promote triplet-pair trapping. This indicates that solely reducing the TT binding energy is not enough to improve TT dissociation rates and that the triplet transfer barrier needs to be also minimized. In this context, similar conclusions were reported for intermolecular TT dissociation in acene-based molecular crystals, for which TT exchange interactions (splitting) and triplet−triplet energy transfer (t) need to be optimized simultaneously to achieve successful triplet-pair separation.[40] It is therefore necessary to determine how to optimize these two features simultaneously in D−A copolymers. We address this question by evaluating the TT dissociation energy and triplet transfer kinetics of a series of extended and minimal D−A prototypes.

First, to establish whether a systematic correlation between the TT splitting and the intramolecular TT-to-$2T_1$ reaction


https://doi.org/10.1021/acs.chemmater.2c00367
Chem. Mater. 2022, 34, 4115−4121

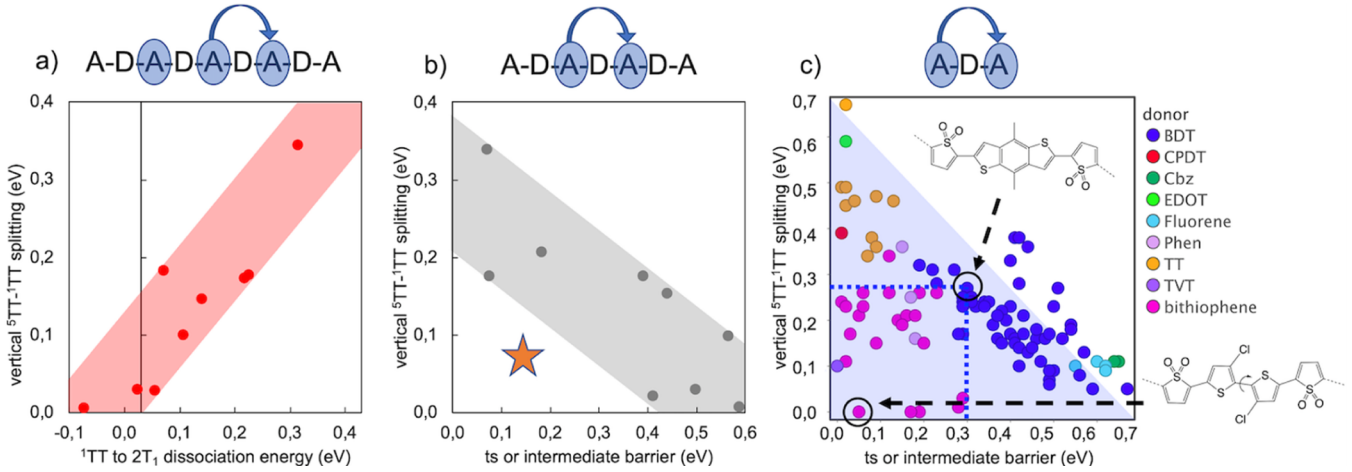


**Figure 4.** (a) Correlation between $^5$TT−$^1$TT vertical splitting and $^1$TT-to-2T$_1$ dissociation energy of the nine D−A copolymers evaluated with the 5A model. (b) Correlation between $^5$TT−$^1$TT splitting and transition state (ts) or intermediate energy barrier associated with the intramolecular energy transfer of a triplet from one acceptor to another, evaluated with the 4A model. The star indicates the optimal region to find systems with a small TT binding energy and triplet transport barrier. (c) Same correlation as in (b) evaluated with the 2A model for a database of 100 A−D−A trimers extracted from ref 32, color-coded with the donor unit. The BDT-TDO and the best candidate are pinpointed and the structure shown. Colored guidelines highlight the trends.

energy exists, these values were computed for nine D−A extended copolymers based on TDO and DPP acceptors (Figure 2). These hold inherently low triplet energies and have been identified as promising building blocks for SF.[29,32,34,35,50,51] The results show that $^1$TT-to-2T$_1$ reaction energies follow opposite trends with respect to the vertical $^5$TT−$^1$TT splitting in a way that larger splitting results in less favorable $^1$TT-to-2T$_1$ thermodynamics (Figure 4a) in agreement with the literature.[36,47] Thus, TT splitting can be used as the reference of TT dissociation energies.

Second, to characterize the triplet-pair dissociation kinetics of these systems, the minimum energy path of the triplet energy transfer process was evaluated from one acceptor to another throughout the donor (i.e., between A−D−$T_1$−D−A−D−A and A−D−A−D−$T_1$−D−A) and compared to that of the TT-to-2T$_1$ dissociation barrier. The results show that the TT-to-2T$_1$ barrier mostly originates from the energy transfer of an isolated triplet (Section S7), and thus the latter can be used to predict the TT dissociation barrier.

For the nine extended D−A copolymers, the correlation between their TT splitting and their triplet transfer barrier shows an unfortunate inversely direct trend in which the cases with the smallest (largest) TT splitting result in the largest (smallest) barriers (Figure 4b). This points to the need for larger-scale sampling of D−A combinations to uncover whether it is indeed possible to find systems in the optimal region, namely, with small TT splitting and triplet transfer barriers, and, thus, to minimize both simultaneously. We took advantage of the 2994 database of D−A dimers previously reported[32] to extract 100 candidates that fulfill the requirements for iSF[33] (Figure 2 and Section S8). For those systems, the TT vertical splitting and triplet energy barrier of their minimal A−D−A model were evaluated. The minimal model slightly overestimates the TT splitting and underestimates the triplet transport barriers but is able to capture the trends of the extended model (Figure S8.1). The results show that the 100 systems spread all over the bottom-left diagonal of the property space but only few have small TT splitting and triplet transfer barriers simultaneously (Figure 4c). Interestingly, the BDT-TDO copolymer prototype lies on the edge of the ∼0.3 eV limit. Analysis of the chemical composition of the systems in the optimal region reveal that these have bithiophene (or TVT in one case) as the donor. In the absence of these two donors, the inversely direct trend between the TT splitting and the triplet transfer barrier is recovered (Figure S8.2). The particularity of these two donors is that they hold inherent flexibility to display coplanar and non-coplanar conformations around they central bond (depending on the electronic state), while the rest are based on conjugated fused rings without this possibility (Figure 2). This inherent flexibility comes from the fact that they are based on two or more covalently bound units with a small rotational barrier. This allows to modulate their coplanarity differently for the TT state minimum, in which the central bond is formally a single bond, and the T$_1$ transition state structure, in which the central bond acquires a double bond character (Scheme 1). The non-coplanarity of the TT

**Scheme 1**

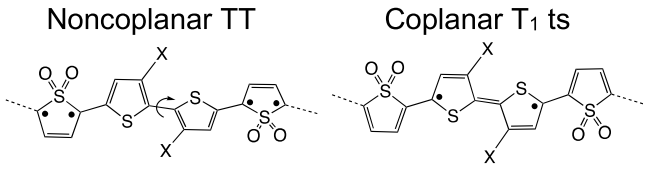


minimum reduces the triplet−triplet interaction and thus the TT binding energy, while the coplanarity of the T$_1$ intermediate (or transition state) tends to reduce the energy barrier.[37,52] For that reason, rigid donors can only minimize one while penalizing the other, (or hold the perfect balance as BDT-TDO) depending on their optimal D−A dihedral. Remarkably, this provides an important extra functionality to the donor unit beyond assisting the S$_1$-to-$^1$TT step of the iSF process, which is to drive the $^1$TT dissociation reaction via intrachain triplet energy transfer. Note that *inter*chain triplet energy transfer would be also possible in polymer thin films.[53,54] This will, however, depend on unpredictable intermolecular arrangements beyond a molecule-based design approach for iSF. In the following, we analyze which features


https://doi.org/10.1021/acs.chemmater.2c00367
Chem. Mater. 2022, 34, 4115−4121

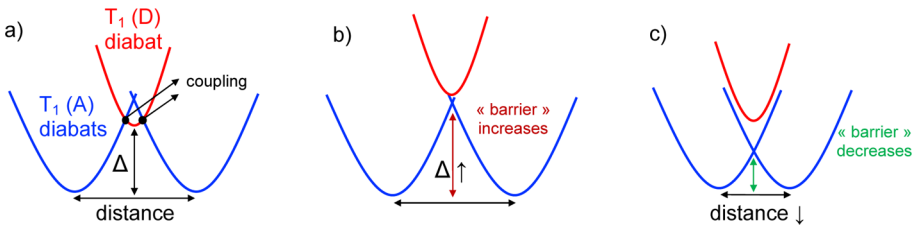


**Figure 5.** Schematic representation of the potential energy profile for intramolecular triplet energy transfer between two acceptors separated by a donor (A−D−A). The blue potentials represent the $T_1$ state of the acceptors and the red potential the $T_1$ state of the donor. The three main features that control the magnitude of the barrier are indicated in (a) the distance between the acceptors, the relative difference between $T_1$ of the donor and the acceptor (labeled Δ), and the coupling between the two, which is partially modulated by the dihedral. The effect of increasing Δ is shown in (b) and of decreasing the distance in (c). Note that the nature of the middle point as an intermediate or transition state would depend on each case.

control the triplet energy transfer barrier throughout the donor and, therefore, the efficiency of the intrachain triplet exciton transport.

Triplet energy transfer is usually described as a bilateral Dexter-type process and is mainly controlled by electronic coupling and inter- (or intra-)molecular distance.[55] Within a Marcus-like potential energy surface perspective,[56] these two features define the position of the transition energy barrier and thus modulate the rate of the triplet exciton transport. In the case of triplet energy transfer between the two acceptors of an A−D−A copolymer, an additional parameter needs to be considered, which is the relative energy difference between the $T_1$ of the donor and the $T_1$ of the acceptor (labeled Δ) (Figure 5). As the distance between the two $T_1$(A) potentials increases, the position of the triplet state of the bridging donor becomes relevant and the middle point becomes an minimum energy intermediate (Figure 5a). This is the case of most of the A−D−A systems based on long donors such as BDT (Table S8.2). In contrast, when the $T_1$(D) energy increases (Figure 5b) and/or the distance between acceptors decreases (Figure 5c), the middle point becomes a transition state. The latter is the case for all phenylene-, thieno[3,2]thiophene- (TT-), or bithiophene-based A−D−A trimers (Table S8.2). The correlation between acceptor−acceptor distance, Δ, and triplet transfer barrier is captured in Figure 6 based on the 100 A−D−A studied systems. On the one side, small barriers (<0.3 eV) are obtained for systems containing small donors (<6.5 Å), while large barriers (>0.3 eV) are obtained for most A−D−A systems containing long donors (>6.5 Å). For exceptionally short donors such as phenylene (red points in Figure 6), the barrier remains small even if the Δ values are as large as 1 eV given that in these cases, the triplet transfer process occurs directly between the two acceptors (as shown in Figure 5c). In addition to the distance and Δ, the dihedral angle plays a non-innocent role in the magnitude of the barrier as mentioned above. The effective conjugation along the A−D−A chain is partially modulated by the coplanarity and as a consequence, systems characterized with the same acceptor−acceptor distance and Δ value tend to display larger (or smaller) barriers for non-coplanar (or coplanar) candidates (Figure S8.3). For that reason, barriers in the 0.2−0.3 eV range can still be obtained for long donors when either Δ or the dihedral is optimal such as in the BDT-TDO case. Clearly, the choice of the donor needs to be made carefully as it will have a direct impact on the triplet-pair separation process and, ultimately, on the iSF conversion rate. Altogether, this adds to the tight list of electronic and structural characteristics required for iSF in D−A copolymers, which include (i) the energetic requirement, by which the energy $S_1$ must be not less than twice the energy of $T_1$, (ii) the coupling requirement, by which $S_1$ needs the CT character to drive efficient $S_1$-to-$^1$TT splitting,[28] and (iii) the separation requirement, by which $T_1$ must be mostly localized in the acceptors.[33] The first and the third conditions were shown to be mainly dependent on the acceptor selection,[33,34] the second on the relative position of the Frontier Molecular Orbitals of the donor and acceptor units[32] and the dihedral between them,[35] and, herein, we recognize the importance of the donor choice (its length, $T_1$ energy, and inherent flexibility) to promote efficient intramolecular triplet-pair separation along the D−A copolymers chain. Future progress in the development of novel D−A combinations with the potential for iSF is envisioned based on these findings.

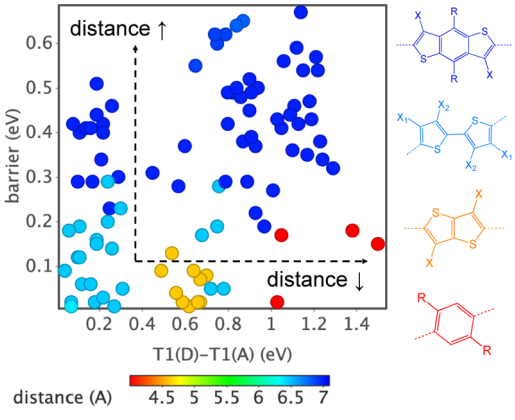


**Figure 6.** Correlation between the $T_1$(D)−$T_1$(A) difference (eV), the acceptor−acceptor distance in Å (which corresponds to the donor length), and the intramolecular triplet transfer barrier (eV) obtained for the 100 A−D−A computed trimers. The molecular structure of an example of each region is shown on the right with the same color.

## CONCLUSIONS

In this work, we exposed the importance of considering triplet exciton transport kinetics, besides $^1$TT thermodynamics, to optimize $^1$TT dissociation rates in extended D−A copolymers for iSF. Our analysis revealed that optimal values for both features can only be achieved when using flexible donors that have at least one rotatable sigma bond leading to a coplanar and a non-coplanar conformation such as bithiophene or TVT, whereas using non-flexible (fused-rings) donors can minimize one while penalizing the other. Using a simple model based on sequential $T_1$ potentials, we discussed the main aspects


https://doi.org/10.1021/acs.chemmater.2c00367
Chem. Mater. 2022, 34, 4115−4121

governing the triplet exciton transport kinetics in A−D−A systems, namely, the acceptor−acceptor distance, the relative energy difference between $T_1$(A) and $T_1$(D), and the degree of coplanarity of the A−D−A chain. Together with the energetic, coupling, and separation requirements previously identified, these additional features can be easily computed and implemented in large-scale high-throughput screening protocols to accelerate the discovery of more efficient D−A copolymer candidates for iSF and, thus, to expand the very limited library of reported systems as of now.

## ■ ASSOCIATED CONTENT

### Supporting Information

The Supporting Information is available free of charge at https://pubs.acs.org/doi/10.1021/acs.chemmater.2c00367.

MS-RASPT2, SF-TDDFT, and RAS-2SF benchmarking; TT dissociation profile of BDT-TDO and BDT-DPP; comparison of TT-to-$2T_1$ and $T_1$-to-$T_1$ barriers; and 100 A−D−A trimer results. All computations reported in this work can be found at https://archive.materialscloud.org/ (PDF)

## ■ AUTHOR INFORMATION


### Corresponding Author

**Clémence Corminboeuf** − *Laboratory for Computational Molecular Design, Institute of Chemical Sciences and Engineering, Ecole Polytechnique Fédérale de Lausanne (EPFL), CH-1015 Lausanne, Switzerland;* orcid.org/0000-0001-7993-2879; Email: clemence.corminboeuf@epfl.ch

### Author

**Maria Fumanal** − *Laboratory for Computational Molecular Design, Institute of Chemical Sciences and Engineering, Ecole Polytechnique Fédérale de Lausanne (EPFL), CH-1015 Lausanne, Switzerland;* orcid.org/0000-0002-4175-8876

Complete contact information is available at: https://pubs.acs.org/10.1021/acs.chemmater.2c00367


### Notes

The authors declare no competing financial interest.

## ■ ACKNOWLEDGMENTS

This work has received support from EPFL and funding from the European Union's Horizon 2020 research and innovation programme under the Marie Skłodowska-Curie grant agreement no. 836849.

## ■ REFERENCES


(1) Smith, M. B.; Michl, J. Singlet Fission. *Chem. Rev.* **2010**, *110*, 6891−6936.

(2) Smith, M. B.; Michl, J. Recent Advances in Singlet Fission. *Annu. Rev. Phys. Chem.* **2013**, *64*, 361−386.

(3) Miyata, K.; Conrad-Burton, F. S.; Geyer, F. L.; Zhu, X.-Y. Triplet Pair States in Singlet Fission. *Chem. Rev.* **2019**, *119*, 4261−4292.

(4) Einzinger, M.; Wu, T.; Kompalla, J. F.; Smith, H. L.; Perkinson, C. F.; Nienhaus, L.; Wieghold, S.; Congreve, D. N.; Kahn, A.; Bawendi, M. G.; et al. Sensitization of Silicon by Singlet Exciton Fission in Tetracene. *Nature* **2019**, *571*, 90−94.

(5) Futscher, M. H.; Rao, A.; Ehrler, B. The Potential of Singlet Fission Photon Multipliers as an Alternative to Silicon-Based Tandem Solar Cells. *ACS Energy Lett.* **2018**, *3*, 2587−2592.

(6) Pazos-Outón, L. M.; Lee, J. M.; Futscher, M. H.; Kirch, A.; Tabachnyk, M.; Friend, R. H.; Ehrler, B. A Silicon−Singlet Fission Tandem Solar Cell Exceeding 100% External Quantum Efficiency with High Spectral Stability. *ACS Energy Lett.* **2017**, *2*, 476−480.

(7) Singh, S.; Stoicheff, B. P. Double-Photon Excitation of Fluorescence in Anthracene Single Crystals. *J. Chem. Phys.* **1963**, *38*, 2032−2033.

(8) Swenberg, C. E.; Stacy, W. T. Bimolecular Radiationless Transitions in Crystalline Tetracene. *Chem. Phys. Lett.* **1968**, *2*, 327−328.

(9) Sanders, S. N.; Kumarasamy, E.; Pun, A. B.; Steigerwald, M. L.; Sfeir, M. Y.; Campos, L. M. Intramolecular Singlet Fission in Oligoacene Heterodimers. *Angew. Chem., Int. Ed.* **2016**, *55*, 3373−3377.

(10) Felter, K. M.; Grozema, F. C. Singlet Fission in Crystalline Organic Materials: Recent Insights and Future Directions. *J. Phys. Chem. Lett.* **2019**, *10*, 7208−7214.

(11) Mora-Fuentes, J. P.; Papadopoulos, I.; Thiel, D.; Alvarez-Boto, R.; Cortizo-Lacalle, D.; Clark, T.; Melle-Franco, M.; Guldi, D. M.; Mateo-Alonso, A. Singlet Fission in Pyrene-Fused Azaacene Dimers. *Angew. Chem., Int. Ed.* **2020**, *59*, 1113−1117.

(12) Schnedermann, C.; Alvertis, A. M.; Wende, T.; Lukman, S.; Feng, J.; Schröder, F. A. Y. N.; Turban, D. H. P.; Wu, J.; Hine, N. D. M.; Greenham, N. C.; Chin, A. W.; Rao, A.; Kukura, P.; Musser, A. J. A molecular movie of ultrafast singlet fission. *Nat. Commun.* **2019**, *10*, 4207.

(13) Pun, A. B.; Asadpoordarvish, A.; Kumarasamy, E.; Tayebjee, M. J. Y.; Niesner, D.; McCamey, D. R.; Sanders, S. N.; Campos, L. M.; Sfeir, M. Y. Ultra-fast intramolecular singlet fission to persistent multiexcitons by molecular design. *Nat. Chem.* **2019**, *11*, 821−828.

(14) Johnson, J. C. Open questions on the photophysics of ultrafast singlet fission. *Commun. Chem.* **2021**, *4*, 85.

(15) Casanova, D. Theoretical Modeling of Singlet Fission. *Chem. Rev.* **2018**, *118*, 7164−7207.

(16) Korovina, N. V.; Joy, J.; Feng, X.; Feltenberger, C.; Krylov, A. I.; Bradforth, S. E.; Thompson, M. E. Linker-Dependent Singlet Fission in Tetracene Dimers. *J. Am. Chem. Soc.* **2018**, *140*, 10179−10190.

(17) Japahuge, A.; Zeng, T. Theoretical Studies of Singlet Fission: Searching for Materials and Exploring Mechanisms. *ChemPlusChem* **2018**, *83*, 146−182.

(18) Reddy, S. R.; Coto, P. B.; Thoss, M. Intramolecular Singlet Fission: Insights from Quantum Dynamical Simulations. *J. Phys. Chem. Lett.* **2018**, *9*, 5979−5986.

(19) Yablon, L. M.; Sanders, S. N.; Miyazaki, K.; Kumarasamy, E.; He, G.; Choi, B.; Ananth, N.; Sfeir, M. Y.; Campos, L. M. Singlet fission and triplet pair recombination in bipentacenes with a twist. *Mater. Horiz.* **2022**, *9*, 462−470.

(20) Ullrich, T.; Munz, D.; Guldi, D. M. Unconventional singlet fission materials. *Chem. Soc. Rev.* **2021**, *50*, 3485−3518.

(21) Padula, D.; Omar, Ö. H.; Nematiaram, T.; Troisi, A. Singlet fission molecules among known compounds: finding a few needles in a haystack. *Energy Environ. Sci.* **2019**, *12*, 2412.

(22) López-Carballeira, D.; Polcar, T. A new protocol for the identification of singlet fission sensitizers through computational screening. *J. Comput. Chem.* **2021**, *42*, 2241−2249.

(23) Musser, A. J.; Maiuri, M.; Brida, D.; Cerullo, G.; Friend, R. H.; Clark, J. The Nature of Singlet Exciton Fission in Carotenoid Aggregates. *J. Am. Chem. Soc.* **2015**, *137*, 5130−5139.

(24) Hu, J.; Xu, K.; Shen, L.; Wu, Q.; He, G.; Wang, J.-Y.; Pei, J.; Xia, J.; Sfeir, M. Y. New insights into the design of conjugated polymers for intramolecular singlet fission. *Nat. Commun.* **2018**, *9*, 2999.

(25) Musser, A. J.; Al-Hashimi, M.; Heeney, M.; Clark, J. Heavy-atom effects on intramolecular singlet fission in a conjugated polymer. *J. Chem. Phys.* **2019**, *151*, 044902.

(26) Aryanpour, K.; Dutta, T.; Huynh, U. N. V.; Vardeny, Z. V.; Mazumdar, S. Theory of Primary Photoexcitations in Donor-Acceptor Copolymers. *Phys. Rev. Lett.* **2015**, *115*, 267401.

(27) Ren, J.; Peng, Q.; Zhang, X.; Yi, Y.; Shuai, Z. Role of the Dark 2Ag State in Donor-Acceptor Copolymers as a Pathway for Singlet Fission: A DMRG Study. *J. Phys. Chem. Lett.* **2017**, *8*, 2175−2181.
(28) Fumanal, M.; Corminboeuf, C. Direct, Mediated, and Delayed Intramolecular Singlet Fission Mechanism in Donor-Acceptor Copolymers. *J. Phys. Chem. Lett.* **2020**, *11*, 9788−9794.
(29) Busby, E.; Xia, J.; Wu, Q.; Low, J. Z.; Song, R.; Miller, J. R.; Zhu, X.-Y.; Campos, L. M.; Sfeir, M. Y. A design strategy for intramolecular singlet fission mediated by charge-transfer states in donor-acceptor organic materials. *Nat. Mater.* **2015**, *14*, 426.
(30) Kasai, Y.; Tamai, Y.; Ohkita, H.; Benten, H.; Ito, S. Ultrafast singlet fission in a push-pull low-bandgap polymer film. *J. Am. Chem. Soc.* **2015**, *137*, 15980−15983.
(31) Grancini, G.; Maiuri, M.; Fazzi, D.; Petrozza, A.; Egelhaaf, H.-J.; Brida, D.; Cerullo, G.; Lanzani, G. Hot exciton dissociation in polymer solar cells. *Nat. Mater.* **2013**, *12*, 29.
(32) Blaskovits, J. T.; Fumanal, M.; Vela, S.; Fabregat, R.; Corminboeuf, C. Identifying the Trade-off between Intramolecular Singlet Fission Requirements in Donor-Acceptor Copolymers. *Chem. Mater.* **2021**, *33*, 2567−2575.
(33) Blaskovits, J. T.; Fumanal, M.; Vela, S.; Corminboeuf, C. Designing Singlet Fission Candidates from Donor-Acceptor Copolymers. *Chem. Mater.* **2020**, *32*, 6515−6524.
(34) Blaskovits, J. T.; Fumanal, M.; Vela, S.; Cho, Y.; Corminboeuf, C. Heteroatom oxidation controls singlet-triplet energy splitting in singlet fission building blocks. *Chem. Commun.* **2022**, *58*, 1338−1341.
(35) Fumanal, M.; Corminboeuf, C. Pushing the Limits of the Donor-Acceptor Copolymer Strategy for Intramolecular Singlet Fission. *J. Phys. Chem. Lett.* **2021**, *12*, 7270−7277.
(36) Kolomeisky, A. B.; Feng, X.; Krylov, A. I. A Simple Kinetic Model for Singlet Fission: A Role of Electronic and Entropic Contributions to Macroscopic Rates. *J. Phys. Chem. C* **2014**, *118*, 5188−5195.
(37) Hasobe, T.; Nakamura, S.; Tkachenko, N. V.; Kobori, Y. Molecular Design Strategy for High-Yield and Long-Lived Individual Doubled Triplet Excitons through Intramolecular Singlet Fission. *ACS Energy Lett.* **2022**, *7*, 390−400.
(38) Wang, Z.; Liu, H.; Xie, X.; Zhang, C.; Wang, R.; Chen, L.; Xu, Y.; Ma, H.; Fang, W.; Yao, Y.; Sang, H.; Wang, X.; Li, X.; Xiao, M. Free-triplet generation with improved efficiency in tetracene oligomers through spatially separated triplet pair states. *Nat. Chem.* **2021**, *13*, 559−567.
(39) Taffet, E. J.; Beljonne, D.; Scholes, G. D. Overlap-Driven Splitting of Triplet Pairs in Singlet Fission. *J. Am. Chem. Soc.* **2020**, *142*, 20040−20047.
(40) Abraham, V.; Mayhall, N. J. Revealing the Contest between Triplet-Triplet Exchange and Triplet-Triplet Energy Transfer Coupling in Correlated Triplet Pair States in Singlet Fission. *J. Phys. Chem. Lett.* **2021**, *12*, 10505−10514.
(41) O'Boyle, N. M.; Banck, M.; James, C. A.; Morley, C.; Vandermeersch, T.; Hutchison, G. R. Open Babel: An open chemical toolbox. *J. Cheminf.* **2011**, *3*, 33.
(42) Chai, J.-D.; Head-Gordon, M. Long-range corrected hybrid density functionals with damped atom-atom dispersion corrections. *Phys. Chem. Chem. Phys.* **2008**, *10*, 6615−6620.
(43) Frisch, M. J.; Trucks, G. W.; Schlegel, H. B.; Scuseria, G. E.; Robb, M. A.; Cheeseman, J. R.; Scalmani, G.; Barone, V.; Mennucci, B.; Petersson, G. A.; et al. *Gaussian 09*, Revision D.01; Gaussian, Inc.: Wallingford, CT, 2009.
(44) Bernard, Y. A.; Shao, Y.; Krylov, A. I. General formulation of spin-flip time-dependent density functional theory using non-collinear kernels: theory, implementation, and benchmarks. *J. Chem. Phys.* **2012**, *136*, 204103.
(45) Casanova, D. Efficient implementation of restricted active space configuration interaction with the hole and particle approximation. *J. Comput. Chem.* **2013**, *34*, 720.
(46) Shao, Y.; Gan, Z.; Epifanovsky, E.; Gilbert, A. T.; Wormit, M.; Kussmann, J.; Lange, A. W.; Behn, A.; Deng, J.; Feng, X. Advances in molecular quantum chemistry contained in the Q-Chem 4 program package. *Mol. Phys.* **2015**, *113*, 184−215.
(47) Feng, X.; Luzanov, A. V.; Krylov, A. I. Fission of Entangled Spins: An Electronic Structure Perspective. *J. Phys. Chem. Lett.* **2013**, *4*, 3845−3852.
(48) Schulten, K.; Karplus, M. On the origin of a low-lying forbidden transition in polyenes and related molecules. *Chem. Phys. Lett.* **1972**, *14*, 305−309.
(49) Brédas, J.-L.; Cornil, J.; Beljonne, D.; Dos Santos, D. A.; Shuai, Z. Excited-state electronic structure of conjugated oligomers and polymers: a quantum-chemical approach to optical phenomena. *Acc. Chem. Res.* **1999**, *32*, 267−276.
(50) Papadopoulos, I.; Álvaro-Martins, M. J.; Molina, D.; McCosker, P. M.; Keller, P. A.; Clark, T.; Sastre-Santos, A.; Guldi, D. M. Solvent-Dependent Singlet Fission in Diketopyrrolopyrrole Dimers: A Mediating Charge Transfer versus a Trapping Symmetry-Breaking Charge Separation. *Adv. Energy Mater.* **2020**, *10*, 2001496.
(51) Shen, L.; Lu, J.; Liu, H.; Meng, Q.; Li, X. Evaluation of Fused Aromatic-Substituted Diketopyrrolopyrrole Derivatives for Singlet Fission Sensitizers. *J. Phys. Chem. A* **2020**, *124*, 5331−5340.
(52) Korovina, N. V.; Chang, C. H.; Johnson, J. C. Spatial separation of triplet excitons drives endothermic singlet fission. *Nat. Chem.* **2020**, *12*, 391−398.
(53) Pace, N. A.; Zhang, W.; Arias, D. H.; McCulloch, I.; Rumbles, G.; Johnson, J. C. Controlling Long-Lived Triplet Generation from Intramolecular Singlet Fission in the Solid State. *J. Phys. Chem. Lett.* **2017**, *8*, 6086−6091.
(54) Tamai, Y.; Ohkita, H.; Benten, H.; Ito, S. Exciton Diffusion in Conjugated Polymers: From Fundamental Understanding to Improvement in Photovoltaic Conversion Efficiency. *J. Phys. Chem. Lett.* **2015**, *6*, 3417−3428.
(55) Dexter, D. L. A theory of sensitized luminescence in solids. *J. Chem. Phys.* **1953**, *21*, 836−850.
(56) Marcus, R. A. Electron transfer reactions in chemistry. Theory and experiment. *Rev. Mod. Phys.* **1993**, *65*, 599−610.


https://doi.org/10.1021/acs.chemmater.2c00367
*Chem. Mater.* 2022, 34, 4115−4121